J Solid State Electrochem (2009) 13:999–1002
DOI 10.1007/s10008-008-0729-6

ORIGINAL PAPER

Measurements of fuel cell internal resistances for the detection of electrode flooding

Hari P. Dhar · Swades K. Chaudhuri

Received: 15 July 2008 / Revised: 6 October 2008 / Accepted: 4 November 2008 / Published online: 21 November 2008

Abstract A clear understanding and the means of prevention of electrode flooding are needed for a durable and commercially viable fuel cell product. Measurements of cell internal resistances, *R*, have proven useful in detecting the onset of flooding. Flooding manifests in the form of a gradual drop in the cell resistance values. For experimental purposes, self-humidified single cells of electrode area 25 cm^2 were built with membrane-electrode assembly (MEAs) made from an experimental lower-Teflon-content gas diffusion layer (GDL) in the micro-porous layer and a commercial GDL sample. To facilitate flooding, favorable conditions, such as lower temperature, air flow, and pressures, were chosen. During the collection of V-I and R-I data, gradual drops in the *R* values were observed in the entire polarization region of the V-I plot. The drop in *R* values is due to the gradual increased hydration level of the Pt/C electrical double-layer interface. At the extreme polarization, the electrode hydration or the flooding of the cell interior is the maximum. Thus, resistance measurement is a viable method for assessing electrode hydration or flooding.

Keywords Fuel cell · MEA · Electrode flooding · Internal cell resistance

Introduction

It is an honor and a pleasure to write this paper to celebrate the 85th birthday of Dr. John O'M. Bockris, adviser and mentor.

H. P. Dhar (✉) · S. K. Chaudhuri
BCS Fuel Cells, Inc., 2812 Finfeather Road,
Bryan, TX 77801, USA
e-mail: info@bcsfuelcells.com

During fuel cell operation, flooding of electrodes can occur. The phenomenon of flooding, as commonly understood, means that some water, which could be either the product of fuel cell reaction or a small portion of the humidification water, is trapped in the matrix of the membrane-electrode assembly (MEA). The matrix construction is gas diffusion layer (GDL)–catalyst–membrane–catalyst–GDL. The trapped water is not easily removed from the matrix by the flows of reactants flowing by the MEA matrix on both sides. The result can be a combination of partial loss of performance with the fuel cell exhibiting cell-variable effects outside the normal range of temperature, pressure, air stoichiometry, and catalyst loading.

Any visually observable effect of flooding involving the gas diffusion sides of the GDL may become noticeable much later—in the course of several weeks or months—in the form of wetting of the GDL macro-porous layer. Only through microscopic examination of the micro-porous layer can changes in the components of the MEA matrix due to flooding be detected. This study concerns the observation of changes in the inner layer through measurements of the cell internal resistances. For comparatively shorter-time experiments, certain conditions of operation can induce quicker flooding. BCS Fuel Cells investigated such conditions during the course of a collection of data points for a V-I curve. More importantly, we investigated conditions of detections of such flooding through measurements of certain properties of the MEA matrix. In this case, we measured cell internal resistances. For the generation of rapid flooding, an experimental GDL with lower Teflon content—more hydrophilic and, therefore, more susceptible to flooding—was chosen and compared with that of a commercial sample.

A number of methods are commonly used for observations of flooding. Frequently, a visual observation is made

of formation and transport of water during the fuel cell reaction. Such techniques have been used by authors in [1–6]. In a variation in the flow visualization, magnetic resonance imaging has been used [7] to follow the flooding. Pressure drop [8–10] and resistance measurements [11] have been also used in following up flooding issues.

To promote the commercialization of fuel cells as a viable and durable alternative clean power source, it is crucial to understand the phenomenon of flooding and to take steps to prevent it.

We report here that internal resistance measurements are capable of detecting the onset of electrode flooding or hydration through gradual drop in internal resistance during the cell polarization measurements.

Experimental

Single self-humidified cells with electrode area of 25 cm^2 were used in the resistance measurements. Catalyst loadings on electrodes were 0.5 mg/cm^2 Pt on the cathode and 0.2 mg/cm^2 Pt on the anode. For this communication, we used two gas diffusion layers: one having 5% Teflon content in the micro-porous layer, and the other a commercial sample with unknown Teflon content in the micro- or macro-porous layers, both obtained from BASF Fuel Cells, NJ, USA. MEAs were made in house with Nafion 212 membrane. All cells were operated self-humidified [12] without any added humidification to either reactant. Cell internal resistances were measured using a computerized instrument from Scribner Associates (model 890C-1kW) having the capability of automatic IR-drop measurements by the technique of current interruption [13].

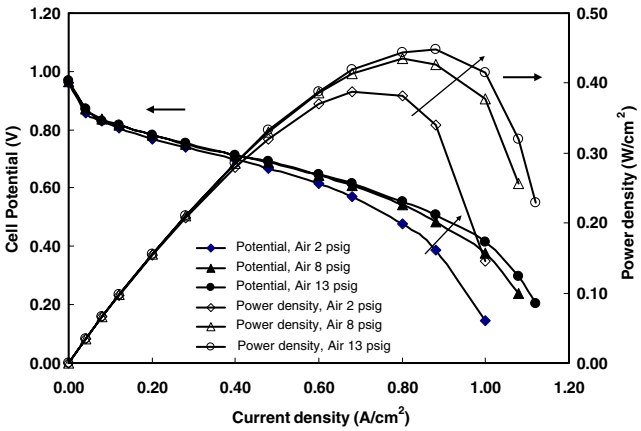

Fig. 1 Performance data of 25-cm^2 single cell with MEA of 5% Teflon content GDL. Air stoichiometry: 1.25, T 40°C, Air P 2–13 psig, H_2 P 2 psig

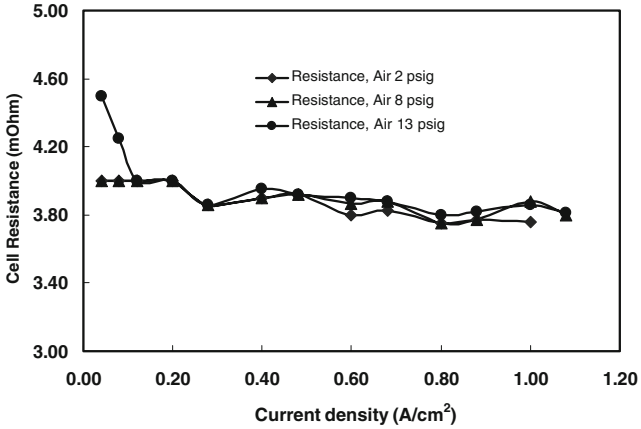

Fig. 2 Internal cell resistance data corresponding to polarization data in Fig. 1

Results

Representative polarization (V-I) and power plot (W-I) data are presented in Fig. 1 for an electrode, designated ETEK#1, with Teflon content of 5% in the micro-porous layer. The air stoichiometry was kept low at 1.25, and air pressure varied at values 2, 8, and 13 psig. Hydrogen pressure was kept constant at 2 psig. Cell temperature was kept constant at 40 °C. These experimental conditions were selected for the easier generation [8, 11] of the flooding of electrode. Since our cell setup operated under conditions of self-humidification, the importance of these experimental conditions was more significant. The data are extended to the extreme mass transfer region, with the cell current reaching up to 1.2 A/cm^2 and the cell potential dropping to about 0.20 V. It is in the mass transfer control region that any observable effect of flooding would be noticed at the initial stage of the onset of electrode flooding. As both the micro- and macro-porous layers become more affected by the flooding, gradually, the effect can become more pronounced in the kinetic and ohmic regions of the polarization plots.

From the polarization plots of Fig. 1, it is not obvious if there is an indication of the flooding startup. Single-cell resistance data as a function of current density for the plot of Fig. 1 are given in Fig. 2. A closer examination of the data reveals that, after a rapid drop at lower currents, there is a gradual almost linear drop in the R values with increasing cell current density, thus generating a negative slope. The absolute value of the slope is about 0.25 mΩ cm^2/A. The average R is about 3.8 mΩ. Figures 3 and 4 present, respectively, the polarization and the resistance data for the commercial GDL sample at two pressures, 2 and 8 psig. Again, the slope in the resistance data is obvious. The slope is about 0.28 mΩ cm^2/A, and the average R is about 4.2 mΩ. Figure 5 presents the resistance data for the commercial sample at various air stoichiometries in the range 1.25 to 1.75 at constant air pressure of 8 psig and

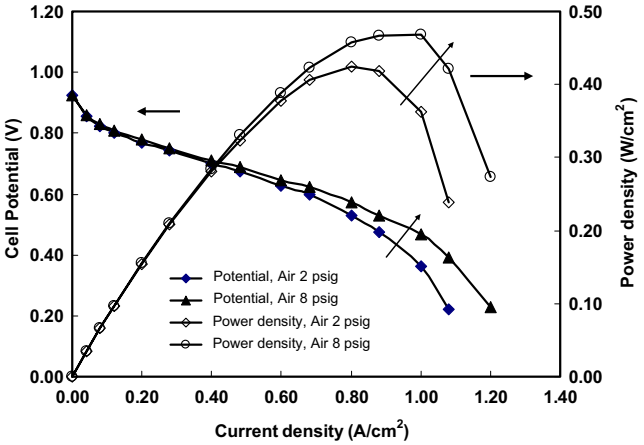

Fig. 3 Performance data of 25-cm^2 single cell with MEA of commercial GDL sample. Air stoichiometry: 1.25, T 40°C, Air P 2–8 psig, H_2 P 2 psig

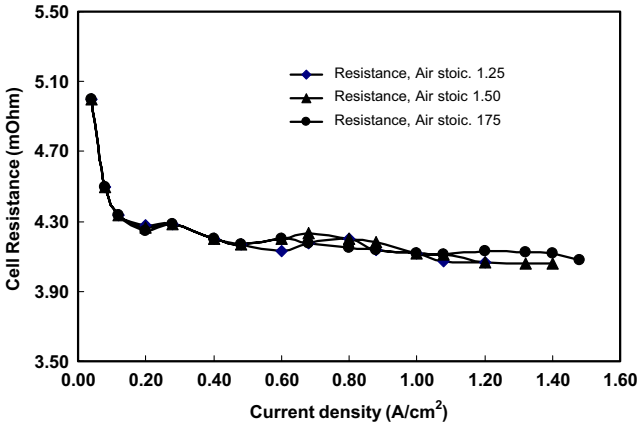

Fig. 5 Internal cell resistance data corresponding to polarization data of the commercial GDL sample operated at air stoichiometries in the range 1.25–1.75, T 40°C, Air P 8 psig, H_2 P 2 psig

hydrogen pressure of 2 psig. Again, *R* decreases gradually with a slope of about 0.25 mΩ cm^2/A with average *R* value of about 4.2 mΩ.

For comparison of the *R* values reported above, we refer to the article by Cooper and Smith [13], who report a value of 0.12 Ω cm^2 for a cell of area 23 cm^2. These numbers give a value of 5.2 mΩ in the same unit we reported above and the cell resistance is in reasonable agreement with ours.

Discussion

As can be observed from Figs. 2, 4, and 5, it is apparent that the cell internal resistance is not constant as a function of polarization current density. It signifies that the *R* changes in the same way in the kinetic, ohmic, and mass transfer control regions of the polarization plot. In the kinetic and ohmic regions, the cell power rises as a function of current density and, in the mass transfer control region, power drops with current density increasing. Only at the start of the polarization is the *R* higher. This is because of the lack of adequate hydration at the electrode interface. Using a similar argument, as the hydration level increases slowly with polarization, the values of *R* keep on dropping slowly. In a fuel cell, the electrode is the Pt/C combination and only prominent ions are H^+ in the matrix of solid electrolyte Nafion. The other prominent component at the electrode interface is H_2O molecule, which is a strong dipole and which can orient at the electrical double layer (cf. [14]) on the electrode interface with oxygen atom towards the positive electrode. The degree of orientation increases with increasing current density. The gradual drop in cell internal resistances can be explained in terms of stronger interaction of the water dipole on the electrode interface. Thus, the increasing hydration effect at the interface can be considered the initial stage of electrode flooding. Flooding can be considered as a fundamental property of the electrode interface related to adsorption and orientation of the water dipole at the electrode interface initially and to the gas diffusion layers when the physical effect of flooding become obvious. The reasons could be insufficient Teflon content in the macro-porous layer and operating under conditions of freeze–thaw cycling, etc.

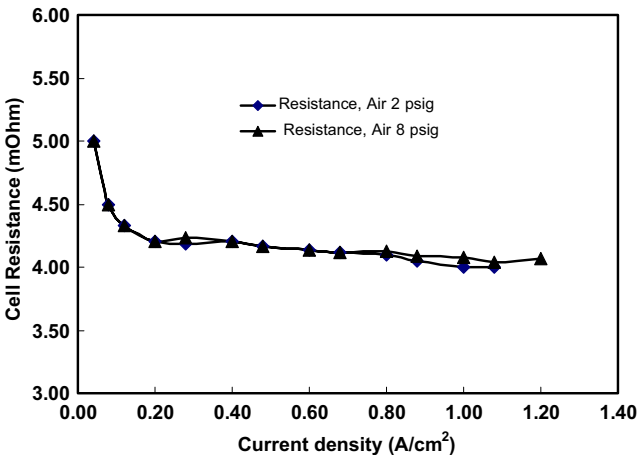

Fig. 4 Internal cell resistance data corresponding to polarization data in Fig. 3

Air pressures and stoichiometries in the ranges examined do not have significant effect on the *R* values. This is consistent with the above explanation that the hydration sheath is not affected by pressure and stoichiometry changes of air.

Resistance of the commercial GDL in the MEA is 4.2 vs. 3.8 mΩ for the lower-Teflon-content GDL in the MEA. These observations suggest that the lower Teflon content in the micro-porous layer allows more hydration and eventually would lead to visual flooding quicker. Noteworthy is that the commercial GDL is also susceptible to hydration and eventual flooding.

The values of slopes of the linear portions of resistance vs. current density plots are very close together suggesting that the rate of drop in R in Figs. 2, 4, and 5 are about the same, and the interfacial hydration progresses at the same rate.

Conclusion

We report here that the onset of electrode flooding or hydration in a fuel cell can be detected with measurements of cell internal resistances. A gradual drop in resistance values occur in the polarization plot covering the kinetic, ohmic, and mass transfer control regions indicating the increasing occurrence of electrode hydration. This is the initial level of electrode flooding, a term commonly used to mean the physical wetting of the macro-porous layers of an MEA. We demonstrate in single cells with MEAs prepared using two GDLs, one experimental of lower Teflon content and the other an actual commercial sample. Experimental conditions were conducive to flooding: lower temperature, lower air flow, and lower air pressures.

Acknowledgement This work was done under subcontract #645 from CFD Research Corporation (prime contract, Department of Energy, Contract No. DE-FG36-07GO17010). The authors acknowledge helpful comments from Dr. Vernon Cole, the program manager at CFDRC.

References

1. Spernjak D, Prasad AK, Advani SG (2007) J Power Sources 170:334. doi:10.1016/j.jpowsour.2007.04.020
2. Su A, Weng FB, Hsu CY, Chen YM (2006) Int J Hydrogen Energy 31:1031. doi:10.1016/j.ijhydene.2005.12.019
3. Liu X, Guo H, Ye F, Ma CF (2007) Electrochim Acta 52:3607. doi:10.1016/j.electacta.2006.10.030
4. Hakenjos H, Muenter U, Wittstadt C, Hebling C (2004) J Power Sources 131:213. doi:10.1016/j.jpowsour.2003.11.081
5. Yang XG, Zang FY, Lubway AL, Wang CY (2004) Electrochem Solid State Lett 7(11):213. doi:10.1149/1.1803051
6. Zhang FY, Yang XG, Wang CY (2006) J Electrochem Soc 152 (2):225. doi:10.1149/1.2138675
7. Minard KR, Viswanathan VV, Majors PD, Wang LQ, Rieke PC (2006) J Power Sources 161:856. doi:10.1016/j.jpowsour.2006.04.125
8. He W, Lin G, Nguyen TV (2003) AIChE J 49(12):3221. doi:10.1002/aic.690491221
9. Barbir F, Gorgun H, Wang X (2005) J Power Sources 141:96. doi:10.1016/j.jpowsour.2004.08.055
10. Tuber K, Pocza D, Hebling C (2003) J Power Sources 124:403. doi:10.1016/S0378-7753(03)00797-3
11. Larminie J, Dicks A (2001) Fuel cell systems explained. Wiley, New York
12. Dhar HP (2005) J Power Sources 143:185. doi:10.1016/j.jpowsour.2004.12.002
13. Cooper KR, Smith M (2006) J Power Sources 160:1088. doi:10.1016/j.jpowsour.2006.02.086
14. Bockris JOM, Devanathan MAV, Muller K (1963) Proc R Soc Lond A274:55